Hydroelastic Response of a Mat-type, Floating Runway near a Breakwater in Irregular Seas

R. Cengiz Ertekin, Jang Whan Kim and Dingwu Xia
Dept. of Ocean Engineering, SOEST, University of Hawaii at Manoa *

Abstract

A wall-sided, shallow rectangular shape is usually considered for floating runways in relatively sheltered locations. The Mega-Float project of Japan is an example to this. Such very large floating structures (VLFS) will be quite flexible under wave action and thus they must be protected by breakwaters. In OCEANS '98 conference, a new approach which is based on the Green-Naghdi theory, was proposed by [1] to determine the dynamic response of a floating runway in the absence of a shoreline or breakwater. The new method was used during a parametric study of a mat-type runway, and it was shown to be much more efficient than other numerical methods routinely used to study the dynamics of conventional-sized offshore structures. In this work, we extend the study of the same problem by including the presence of a breakwater, and to irregular seas defined by a spectral formula. We also refine the numerical model that was used before. The numerical efficiency is improved further by adopting the eigenfunction expansion method of [2]. Using this improved model, the response amplitude operators and motion response spectra of the runway displacement are obtained in the presence of a breakwater and in long-crested random seas.

I- Introduction

Mat-type floating runways are generally planned to be located near shore and protected by breakwaters. To determine an optimal location of the floating runway and breakwater, one needs an efficient numerical tool to estimate the hydroelastic response of the runway in deterministic and random waves.

The hydroelastic response of a floating mat has typically been treated by panel methods in the frequency domain. The floating runway is modeled as either a three-dimensional elastic body, see [3], or a thin elastic plate, see [4], [5], and the entire surface of the elastic body is discretized into panels to obtain the hydrodynamic coefficients for assumed modes of elastic deformation or to couple the fluid and structure directly. Because the length of the incident wave is smaller than the runway length and, in some cases, even its beam, one needs a large number of modes and panels to obtain sufficient accuracy. If we denote the length ratio between the runway-length and wavelength scales as N, the number of unknowns is $O(N^2)$ and the number of Green-function evaluations is $O(N^4)$ when we use a panel method. This presents difficulties in using the panel methods as quantitative analysis tools for design. If one further needs to consider the interaction of the floating structure with a shoreline and breakwater, then it is doubtful that a conventional panel method can be used for design purposes.

In this study, we use a numerical method where the number of unknowns is reduced to $O(N)$ and the Green-function evaluations to $O(N^2)$. Furthermore, the Green function used in the present method is much simpler than the one used in panel methods. With this improved numerical efficiency, this method has been successfully applied to the response of floating runways in open seas in [1], [6] and near a shoreline in [7], and proven to be efficient and effective in parametric studies of floating runways. In this paper, we apply the new method to the hydroelastic response of a floating runway sheltered by a breakwater.

We take advantage of the high length-to-depth ratio of the mat-type structure and the fluid layer underneath in the present method. The floating runway and the fluid layer is modeled by the thin-plate theory and the Green-Naghdi (GN) theory, respectively, the details of which can be found in [8] and [9], respectively. When the equations from the two theories are coupled, we can obtain equations similar to the ones given in [10], but with an improved dispersion relation, as shown in [11]. The coupled equations can be factored into three Helmholtz equations, whereas the wave motion in the outer domain is governed by one Helmholtz equation. The Helmholtz equation in the outer domain can effectively be solved using the Green-function method, where the solutions are given as line integrals along the edge of the runway and the breakwater. In the inner region covered by the mat, rather than using the integral equation method as in [1] and [6], a more efficient eigenfunction expansion method is adopted from [2]. The Green functions for

*2540 Dole Street, Holmes Hall 402, Honolulu, HI 96822, USA.

these equations can simply be given as Hankel functions. As a result, the computational cost for the hydroelastic analysis of floating runways can now be comparable to that used for analysis of harbor oscillations, which has been readily applied for practical use since the early 70's (see e.g., [12]).

The method developed is then applied to a 5-km-long floating runway by fixing its length, beam, draft and rigidity. Computations are made for incoming wavelengths from 100 m to 500m. Short-term extreme response (vertical displacement) amplitudes are also obtained for the significant wave heights of 4m and 8m by using the two-parameter Bretschneider spectrum. The results show, in most cases, that the presence of the breakwater affects the deflections favorably. Exceptions have been found when the wave direction is parallel to the breakwater; an increase in runway deflection of up to 40% is observed along the centerline of the runway in this case. This phenomenon can be explained by trapping of waves between the runway and breakwater.

II- **Boundary-Value Problem**

An elastic mat of rectangular plan geometry, with length, L, beam, B, and draft d is considered, see Fig. 1. The mat is freely floating on an inviscid fluid-layer of constant density ρ and depth h, and is under the action of linear shallow-water waves of angular frequency ω and direction β. The origin of the Cartesian system $Oxyz$ is placed at the center of the runway. The breakwater is defined by a finite length, L_b, at $y = -B/2 - S$, and constant thickness B_b, at a distance of S from the breakwater-side edge of the runway, and it extends to the sea floor with vertical sides . Two regions which describe the fluid region (I) and the fluid-plate region (II) are considered, and these regions are separated by the juncture boundary J.

We assume that the wavelength, λ, of the incoming waves is much larger than the wave amplitude, A, and water depth (or $kA \ll 1, kh \ll 1$, where k is the wave number), such that we can use the linear Green-Naghdi theory (Level I) to model the motion of the fluid layer. We also assume that the thickness of the mat is much smaller than the length and beam of the mat so that we can employ the thin-plate theory that governs the hydroelastic deflections of the mat.

Within the scope of the linear theory, the motions of the plate and fluid can be assumed time harmonic with the same angular frequency, ω, of the incoming waves. Hereafter, we will represent any time-harmonic function, say $f'(x, y, t)$, as the real part of $f(x, y)e^{-i\omega t}$ by introducing a complex function, $f(x, y)$ that depends on the spatial variables only.

The rectangular mat is assumed to have a uniform mass distribution (per unit area), m, and flexural rigidity (per unit width), $D = EI/B$, where E is Young's modulus and I is the moment of inertia of plate cross section. The vertical displacement, $\zeta(x, y)$, of the mat is assumed to be governed by the thin-plate theory (see e.g., [8]):

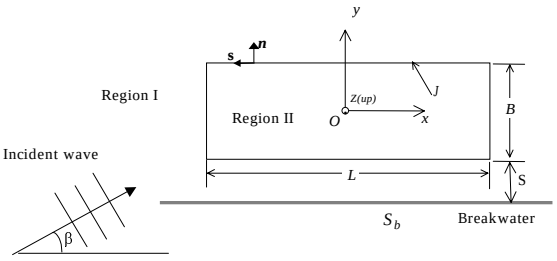

(a) Plan view

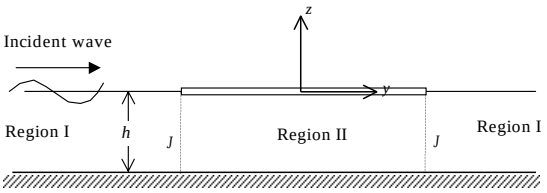

(b) Side view

Figure 1: Definition sketch of the problem.

$$-m\omega^2\zeta + D\Delta^2\zeta = p_f, \tag{1}$$

where $p_f = p_f(x, y)$ is the spatial part of the time-harmonic pressure on the bottom of the plate and $\Delta = \partial^2/\partial x^2 + \partial^2/\partial y^2$ is the two-dimensional Laplacian on the horizontal plane.

Since the plate is freely floating, the bending moment and shear force should vanish at the edges of the plate:

$$\begin{aligned} \Delta\zeta - (1-\nu)\frac{\partial^2\zeta}{\partial s^2} &= 0, \\ \frac{\partial}{\partial n}\left\{\Delta\zeta + (1-\nu)\frac{\partial^2\zeta}{\partial s^2}\right\} &= 0 \quad \text{on} \quad J, \end{aligned} \tag{2}$$

where n and s denote the normal and tangential directions as seen in Fig. 1, and ν is Poisson's ratio.

At the corners of the plate, there can be concentrated shear force to compensate for the torsional moment along the edges of the plate. The vanishing of this shear force leads to

$$\frac{\partial^2\zeta}{\partial x \partial y} = 0 \quad \text{at} \quad x = \pm\frac{L}{2} \ \text{ and } \ y = \pm\frac{B}{2}. \tag{3}$$

For the fluid motion, we assume that the linear, Level I GN equations govern the time-harmonic fluid motion. The horizontal velocity field $\mathbf{V}(x,y)$ and the vertical velocity component $w(x,y,z)$ are given in terms of the mean velocity potential $\psi(x,y)$ (see [11]):

$$\begin{aligned} \mathbf{V}(x,y) &= \nabla\psi(x,y), \\ w(x,y,z) &= -i\omega\zeta(x,y)\frac{z+h}{h}. \end{aligned} \tag{4}$$

With this representation of the velocity field, the combined mass and momentum equations for the linear, Level I GN equations become

$$\Delta\psi + k^2\psi = \frac{k^2}{i\omega\rho}p_f, \tag{5}$$

where the wave number, k, is given by

$$k^2 = \frac{3\omega^2}{3gh - h^2\omega^2} \quad \text{or} \quad \omega^2 = \frac{3ghk^2}{3 + h^2k^2}. \tag{6}$$

The spatial part of the fluid-top-surface displacement in the fluid region or the fluid-plate region is given by a complex function:

$$\zeta = \frac{h}{i\omega}\Delta\psi. \tag{7}$$

And the depth integrated pressure $P(x,y)$ is given by

$$P(x,y) = i\omega\rho h\psi. \tag{8}$$

In Region I, the atmospheric pressure is neglected without loss in generality, i.e., $p_f = 0$, and therefore, we have

$$\Delta\psi_I + k^2\psi_I = 0, \tag{9}$$

as the governing equation. On the the surface of breakwater, S_b, ψ_I should satisfy the no-flux condition:

$$\frac{\partial\psi_I}{\partial n} = 0, \quad \text{on } S_b \tag{10}$$

In Region II, if we couple the equations of motion of the plate, (1), and the fluid, (5), we obtain the following governing equation:

$$\begin{aligned} D\Delta^3\psi_{II} + \rho g\Delta\psi_{II} - \left(m + \frac{\rho h}{3}\right)\omega^2\Delta\psi_{II} \\ + \frac{\rho\omega^2}{h}\psi_{II} = 0. \end{aligned} \tag{11}$$

Boundary conditions should also be provided on other boundaries: i) the juncture, J, boundary condition for continuity, and ii) the radiation condition at infinity. Along the juncture boundary, J, the continuity of mass flux and depth-mean pressure leads to the following matching conditions:

$$\frac{\partial\psi_I}{\partial n} = \frac{\partial\psi_{II}}{\partial n}, \qquad \psi_I = \psi_{II} \quad \text{on } J, \tag{12}$$

and these conditions will couple the solutions of equations (9) and (11) as we will discuss in detail in the next section. The radiation condition has to be imposed on part of ψ_I; this will also be discussed in the following section.

III- **Method of Solution**

A- *Decomposition of the hydroelastic problem*

The governing equation in Region I, (9), is the well known Helmholtz equation whose solution can be represented by a boundary integral along J, as will be shown later. On the other hand, the governing equation in Region II, (11), is more complicated. Fortunately, however, we can decompose equation (11) into three Helmholtz-type equations by factorizing the differential operators as shown by [6].

The boundary-value problem in Region II can then be decomposed as

$$\psi_{II} = \psi_0 + \psi_1 + \psi_2, \tag{13}$$

where ψ_j, $j = 0, 1, 2$, satisfy the following equation in Region II:

$$(\Delta - \mu_j^2)\psi_j = 0, \tag{14}$$

where μ_j are the roots of the characteristic equation of (11). By defining a real, positive number k_p such that $k_p^2 = -\mu_0^2$, equation (14) for $j = 0$ can be written as

$$(\Delta + k_p^2)\psi_0 = 0, \tag{15}$$

which is the Helmholtz equation for the hydroelastic waves in Region II. The other two equations for $j = 1, 2$ give the evanescent solutions trapped near the edges of the plate.

From equations (7), (13) and (14), the plate displacement ζ is obtained as

$$\zeta = \frac{h}{i\omega}\sum_{j=0}^{2}\mu_j^2\psi_j \tag{16}$$

Then the free-edge conditions, (2), can be written in terms of μ_j and ψ_j.

In the fluid region, Region I, the general solution can be decomposed into the incoming wave potential, ψ_w, and the disturbance potential ψ_3, i.e.,

$$\psi_I = \psi_w + \psi_3, \tag{17}$$

where ψ_w is well known.

The potential ψ_3 represents the sum of the diffraction and radiation (which is due to the hydroelastic motions of the plate) potentials. On the breakwater, ψ_3 should satisfy the no-flux condition:

$$\frac{\partial \psi_3}{\partial n} = -\frac{\partial \psi_w}{\partial n}, \quad \text{on } S_b \tag{18}$$

In the far field, ψ_3 must also satisfy the Sommerfeld radiation condition.

The matching conditions (12) can now be written as

$$\sum_{j=0}^{2} \frac{\partial \psi_j}{\partial n} - \frac{\partial \psi_3}{\partial n} = \frac{\partial \psi_w}{\partial n}, \tag{19a}$$

$$\sum_{j=0}^{2} \psi_j - \psi_3 = \psi_w \quad \text{on } J. \tag{19b}$$

B- *Solutions of the Helmholtz equations*

The hydroelastic problem to be solved is designated by four Helmholtz equations for ψ_0, ψ_1, ψ_2 and ψ_3. The first three Helmholtz equations are defined in a bounded rectangular region and can easily be solved using the separation of variables technique. On the other hand, the Helmholtz equation in the outer domain can be treated more easily by the Green-function method. Following [2], we write $\psi_m \quad (m = 0, 1, 2)$ as eigenfunction series with unknown coefficients to be determined. The series expansions of ψ_m satisfy the governing equations, (14), and the corner conditions, (3).

In the outer domain, we write ψ_3 as a line source distribution of the Green function along the edges of the runway, J, and breakwater, S_b. To do this, we divide the contour $J \cup S_b$ into a finite number of segments, $I_1, I_2, \ldots, I_{N_p}$.

Assuming that the source strength is constant on each segment, and defining the arc length coordinate s along $J \cup S_b$, we can write

$$\psi_3(x, y) = \sum_{n=1}^{N_p} \sigma_n \int_{I_n} G(\mathbf{x}; \boldsymbol{\xi}(s))\, ds, \tag{20}$$

where $\mathbf{x} = (x, y)$ is the field point and $\boldsymbol{\xi}(s) = (\xi(s), \eta(s))$ is the source point on $J \cup S_b$, and $G(\mathbf{x}; \boldsymbol{\xi})$ is the Green function given in terms of the Hankel function (or Weber's solution).

The solutions satisfy the governing equations and the boundary conditions except the free-edge conditions given in (2) and the matching conditions in (19a, b). Following [2], the conditions (2) and (19a) are weakly satisfied by taking the inner-product with the cosine modes along all four edges of the runway. On the other hand, the matching condition (19b) is satisfied at the midpoints $\mathbf{x}_i = (x_i, y_i)$ of each segment I_i, placed along the edges of runway. The reader is referred to [2] for further details of the solution procedure.

C- *Irregular-sea analysis*

The random-sea response of the runway will be determined by assuming that the waves are long-crested, although the short-crested wave case follows in a straight forward manner. For a narrow-banded spectrum, the wave heights follow the Rayleigh probability distribution, and thus the significant response, R_s, is twice the standard deviation of the response. The short-term extreme amplitude response, R_e, of runway deflections, for 1-in-1000 maximum event, is then given by

$$R_e = 1.86 R_s = 3.72 \sqrt{m_0}, \tag{21}$$

where $m_0 = \int_0^\infty H^2(\omega) S_\eta(\omega)\, d\omega$, $H(\omega)$ is the transfer function (or response amplitude operator as used here) of the deflection, i.e., $H(\omega) = |\zeta|/A$, and $S_\eta(\omega)$ is the incoming-wave spectrum. We use the two-parameter Bretschneider spectrum (see e.g., [13]) in the calculations for the two irregular sea states that correspond to the significant wave height and peak period pairs of $H_s = 4m, T_p = 13s$ and $H_s = 8m, T_p = 16s$, see Fig. 2.

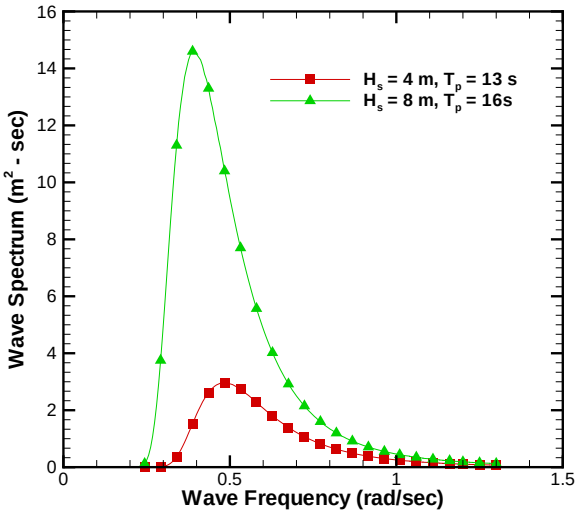

Figure 2: Bretschneider spectra for the two sea states.

These approximate Sea States 6 and 7, and they were chosen to make sure that there is insignificant wave energy at the small wave periods of about 8s and below so that the linear GN equations would not loose their applicability; see [14] for a discussion on the subject. In fact, we see from (6) that, as $kh \to \infty$, the wave frequency has a cut-off value, namely that $\omega \to 3g/h$. In the application of the method discussed next, we assume

that the water depth is $h = 50$m, so that, as $kh \to \infty$, $\omega \to 0.7672$rad/s or wave period goes to $T \to 8.2$s.

IV- APPLICATION AND DISCUSSION

To show the effects of a breakwater on the wave-induced response of a floating runway, we consider the behavior of a VLFS both in open seas (meaning, in the absence of any other 'structure', such as a breakwater, or a shoreline), and near a breakwater. The main dimensions, water depth and the material properties are given as $L = 5$km, $B = 1$km, $d = 5$m, $h = 50$m, $D = 1.96 \times 10^{11}\mathrm{N} - \mathrm{m}$. The same runway has been studied in open seas in [5], [6], and in the presence of a shoreline in [7]. We set the length and thickness of the breakwater as $L_b = 6$km and $B_b = 25$m. The breakwater can be seen in Fig. 5a,c,e.

In the computations, the length of the segments, $I_{1,2,\ldots,N_p}$, was chosen such that there is at least ten segments in one wave length. The number of eigenfunctions, N_x and N_y, was taken as 1/4th of the number of segments along the longitudinal and transverse edges of the runway, respectively, based on the experience gained by the numerical experiments of [2]. Several schemes have been introduced to enhance the efficiency of the numerical method further. Since the edge of the runway and breakwater are straight lines and are parallel to each other (this is not a necessary condition in the present method which is general), the evaluation of the line integral given in (20) can be optimized if we use the same length for the line segments to discretize the edges. Then the cost for the evaluation of the Green function can be reduced from $O(N^2)$ to $O(N)$.

Numerical computations are carried out using a Pentium II PC/450MHz. When $T = 9$s or $L/\lambda = 40$, the CPU time to evaluate the hydroelastic response of the runway for 181 wave angles, 0^o to 90^o by 0.5^o increments, was 29min 20s when we used 960 line segments in open seas. With the breakwater, we used 1924 segments, and the CPU time was 1hr. Although it is difficult to make a direct comparison due to the difference in the computers used, the computational time of 7hr without a breakwater and 21hr with a breakwater were reported by [15], where a higher-order boundary-element method was used to analyze a 1600m $\times$ 400m floating runway.

We investigated the hydroelastic response of the runway for wave periods, T, varying between 8s and 24s, wave angles, β, varying between 0^o and 90^o, and $S = 500$m. In the present method, we can obtain the deflections at any point on the plate. However, the deflections along the centerline ($|x| \leq 0.25L, y = 0$) of the runway, where the take-off and landing operations would take place, and at the four corners, where the hydroelastic deflections are most severe, are of particular concern.

The overall hydroelastic response amplitude operators (deflection amplitude per unit wave amplitude)of the runway for $8s \leq T \leq 24s$ and $0^o \leq \beta \leq 90^o$ are shown by surface-contour plots in Figs. 3 and 4 for the breakwater distance of $S = 500$m. Note that the vertical scales of the plots are different in Figs. 3 and 4. It is seen that the runway is well protected by the breakwater when $\beta > 15^o$. When $\beta \leq 15^o$, the presence of the breakwater increases the deflection amplitudes on the runway, especially at the lower-right corner. The steep hills seen in the plots of Figs. 3a and 4a, which are due to the trapping of hydroelastic waves near the critical wave angle, were explained by [6] and [11]. These hills mostly disappear when we consider the presence of the breakwater as seen in Figs. 3b and 4b. The significant increase in deflections at the lower-right corner could also be found along the runway edge facing the breakwater. Also observed is the increase in the relative wave height at this edge, which indicates once more that the increased response is due to wave trapping between the runway and breakwater.

The contour plots of the deflections on the runway and the wave elevation around the runway and breakwater, for $T = 14s$, is shown in Fig. 5. Again, the runway is well protected in both the beam and quartering seas. When $\beta = 0^o$ and there is no breakwater, the hydroelastic waves on the runway attenuate as they propagate along the length of the runway due to the radiation of the gravity waves along the side edges of the runway. When the breakwater is present, the radiated waves bounce back to the runway and then back to the breakwater again, and so forth. As a result, the gravity waves are trapped in the 'trench' between the runway and breakwater, and prevent the attenuation of the hydroelastic waves by building trapped edge-waves along the runway.

The RAOs obtained for the vertical displacements of the runway can be used to determine the significant and short-term extreme responses in irregular waves as explained before. The short-term extreme amplitude values of the vertical displacements of the runway at the lower-right corner and along (maximum value was chosen) the center-line of the runway for the two sea states are shown in Figs. 6 and 7, respectively. In these bar charts, the darker bars denote the results obtained when there is a breakwater 500m away from the runway.

As it has already been shown in [1], [2], [6] and [7], the vertical displacements of the runway in the absence of a breakwater are unacceptably large. The present results leads to the same conclusion in irregular waves, namely that a mat-type VLFS must be protected by one or more breakwater(s). From Figs. 6 and 7, and as also mentioned before, the breakwater essentially amplifies the deflections when the wave incidence angle is $\beta \leq 15^o$,

and therefore a second breakwater to the left of the runway (see Fig. 1) must be placed to reduce the deflections to an acceptable level.

V- CONCLUSIONS

In this study, an efficient numerical method based on the linear Green-Naghdi theory is developed to investigate the hydroelastic response of a mat-type VLFS sheltered by a breakwater in regular and irregular waves. The computations show that this method is much more efficient than the conventional panel methods. The numerical simulations are carried out for a wide range of wave angles and wave lengths. The results indicate that the structure is well protected by the breakwater except when the wave incidence angle is less than about 15^o. At these small wave incidence angles, significant increases in deflections along the edge of the runway, facing the breakwater, are observed due to wave trapping between the runway and breakwater. It is concluded that a mat-type VLFS operating in restricted waters must be protected by breakwaters.

Acknowledgment: The material is based upon work supported by the U.S. National Science Foundation, Grant No. BES-9532037, and by the U.S. Office of Naval Research's MOB Program. SOEST Contribution No. 4828.

References

[1] R. C. Ertekin and J. W. Kim. A parametric study of the hydroelastic response of a floating, mat-type runway in regular waves. In *OCEANS '98 Conference*, page 5pp., Nice, France, September 1998. IEEE.

[2] J. W. Kim and R.C. Ertekin. An eigenfunction-expansion method for predicting hydroelastic behavior of a shallow-draft VLFS. In *Second Int. Conf. On Hydroelasticity in Marine Technology (Hydroelasticity '98)*, pages 47–59, December 1998.

[3] S. Q. Wang, R. C. Ertekin, and H. R. Riggs. Computationally efficient techniques in the hydroelasticity analysis of very large floating structures. *Computers and Structures*, 62(4):603–610, 1997.

[4] M. Mamidipudi and W. C. Webster. The motions performance of a mat-like floating airport. In O. M. Faltinsen, editor, *Hydroelasticity in Marine Technology*, pages 363–375. Balkema Publishers, Rotterdam, 1994.

[5] M. Kashiwagi. A B-spline Galerkin scheme for calculating the hydroelastic response of a very large floating structure in waves. *J. Mar. Sci. Tecnol.*, 3:37–49, 1998.

[6] R. C. Ertekin and J. W. Kim. Hydroelastic response of a mat-type structure in oblique, shallow-water waves. *To appear in J. Ship Res.*, 1999.

[7] D. Xia, J. W. Kim, and R.C. Ertekin. The effect of shoreline proximity on the hydroelastic response of a floating runway. In *18th Int. Conf. on Offshore Mechanics and Arctic Engineering*, page 8pp. ASME, July 1999.

[8] J. W. S. Rayleigh. *The Theory of Sound.* Dover Publications (1945), New York, 1894.

[9] R. C. Ertekin. *Soliton Generation by Moving Disturbances in Shallow water: Theory, Computation and Experiment.* PhD thesis, U.C. Berkeley, May 1984.

[10] J. J. Stoker. *Water Waves: The Mathematical Theory with Applications.* New York: Interscience, 1957.

[11] J. W. Kim and R. C. Ertekin. Deformations of an infinitely-long, elastic plate floating in oblique waves: Linear Green-Naghdi theory. *Submitted to J. Fluid Mech.*, 1999.

[12] V. W. Harms. Diffraction of water waves by isolated structures. *J. Waterway, Port, Coastal and Ocean Div.*, ASCE, 105(WW2):131–147, 1979.

[13] S. K. Chakrabarti. *Hydrodynamics of Offshore Structures.* Computational Mechanics Publications, Boston, 1987.

[14] R. C. Ertekin and J. M. Becker. Nonlinear diffraction of water waves by a submerged shelf in shallow water. *J. Offshore Mech. & Arctic Engng.*, 120:212–220, November 1998.

[15] Utsunomiya, E. T., Watanabe, and R. E. Taylor. Wave response analysis of a box-like VLFS close to a breakwater. In *17th Int. Conf. on Offshore Mechanics and Arctic Engineering*, page 8pp. ASME, OMAE98-4331, July 1998.

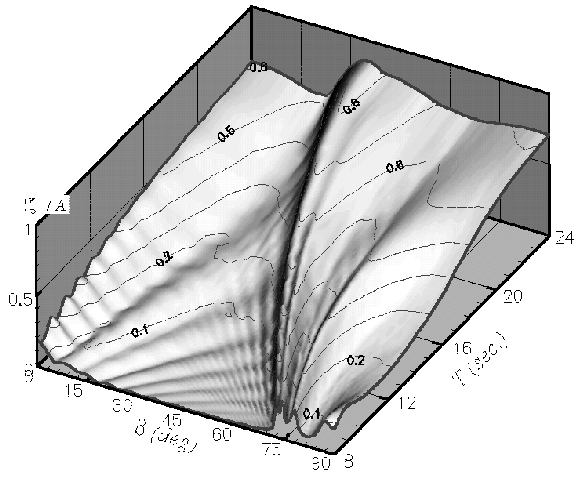

(a) Without breakwater

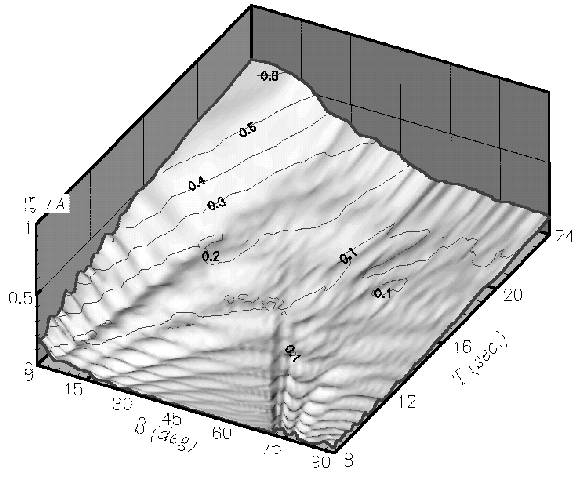

(b) With breakwater

Figure 3: Surface-contour plots of maximum runway deflections along the center-line, $S = 500$m.

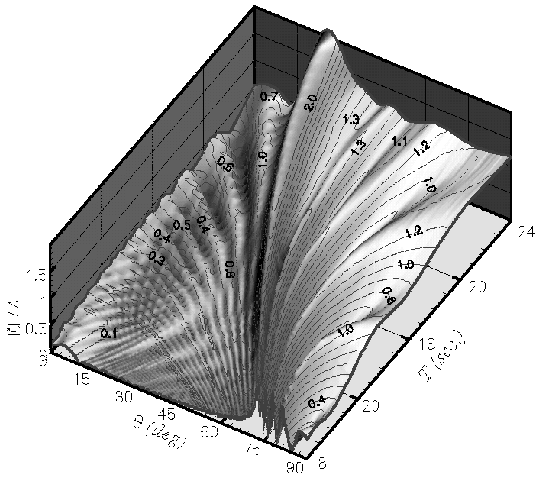

(a) Without breakwater

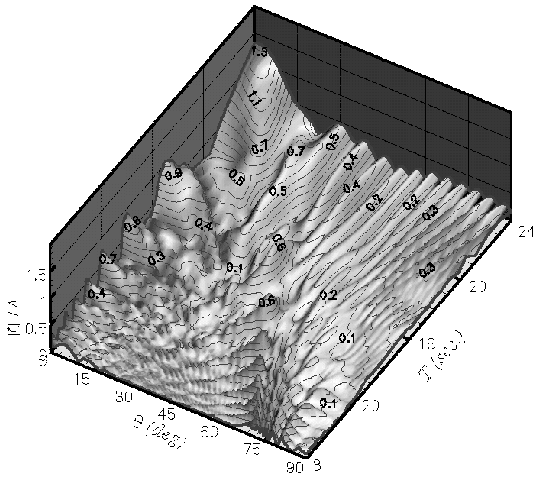

(b) With breakwater

Figure 4: Surface-contour plots of runway deflections at the lower-right corner, $S = 500$m.

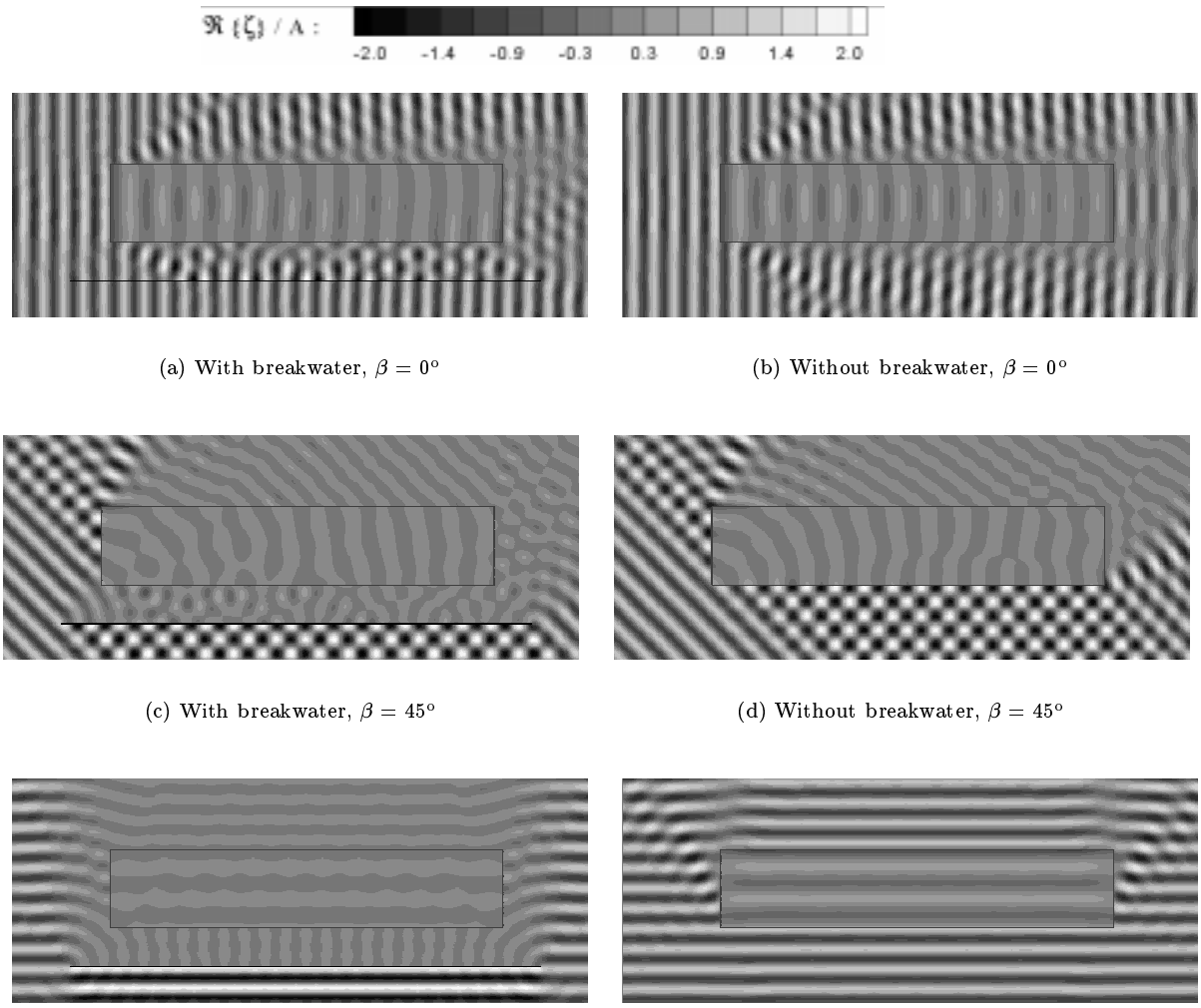

(a) With breakwater, $\beta = 0^o$

(b) Without breakwater, $\beta = 0^o$

(c) With breakwater, $\beta = 45^o$

(d) Without breakwater, $\beta = 45^o$

(e) With breakwater, $\beta = 90^o$

(f) Without breakwater, $\beta = 90^o$

Figure 5: Contour plots of $\Re\{\zeta\}/A$: $T = 14s$. The breakwater in (a),(c) and (e) is placed at 500m from the runway.

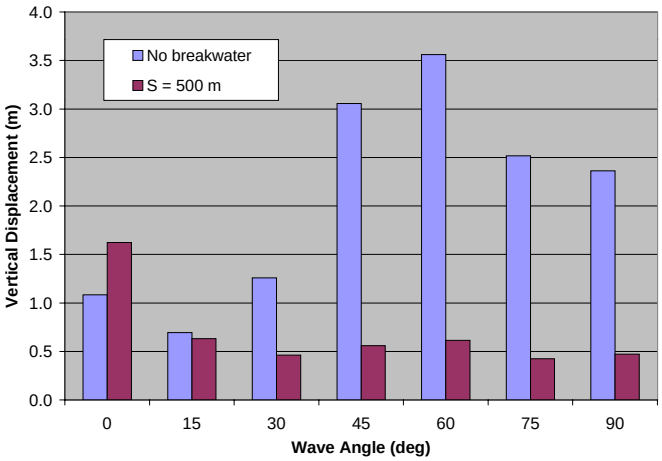

(a) Lower-right corner

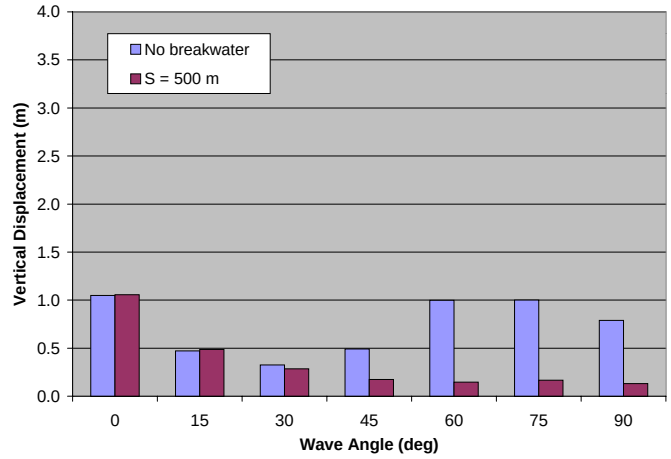

(b) Maximum along the centerline, $-L/4 < x < L/4$

Figure 6: Extreme vertical displacement amplitudes for $H_s = 4\text{m}, T_p = 13\text{s}$.

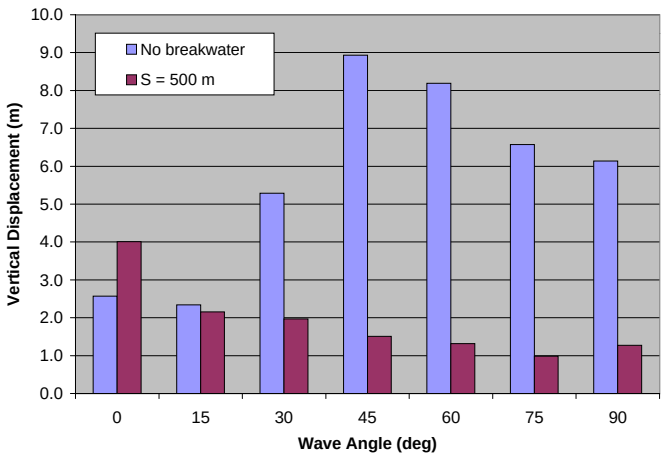

(a) Lower-right corner

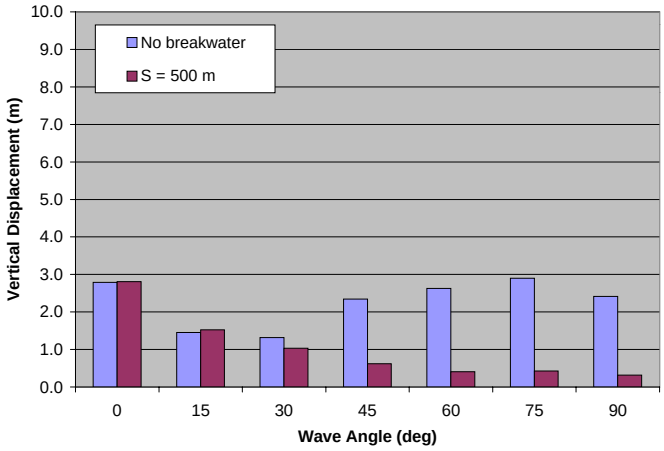

(b) Maximum along the centerline, $-L/4 < x < L/4$

Figure 7: Extreme vertical displacement amplitudes for $H_s = 8\text{m}, T_p = 16\text{s}$.